Dual Theory of Turbulent Mixing

Alexander Migdal
Institute for Advanced Study, Princeton, NJ, USA

(*Electronic mail: amigdal@ias.edu)

(Dated: May 14, 2025)

We present an exact analytic solution for incompressible turbulent mixing described by 3D NS equations, with a passive scalar (concentration, temperature, or other scalar field) driven by the turbulent velocity field. Using our recent solution of decaying turbulence in terms of the Euler ensemble, we represent the correlation functions of a passive scalar as statistical averages over this ensemble. The statistical limit, corresponding to decaying turbulence, can be computed in quadrature, by a multi-dimensional Mellin-Barnes integral representation. We find the decay spectrum and the scaling functions of the pair correlation. Full comparison with physical and real experiments is postponed till the future detailed computation of the spectrum in our solution.

Keywords: Turbulence, Fractal, Fixed Point, Velocity Circulation, Loop Equations

I. INTRODUCTION

Turbulent mixing, the process of advecting and diffusing a passive scalar by a turbulent velocity field, is integral to numerous natural and technological phenomena, ranging from atmospheric dispersion to oceanographic processes and industrial mixing[1–3]. The essence of turbulent mixing lies in the interplay between the advective action of turbulent flows and molecular diffusion[4,5]. This introductory section summarizes the role of turbulent mixing across disciplines and reviews the current theoretical, experimental, and numerical understanding, primarily focusing on passive scalar mixing in turbulent flows as discussed in a review paper by Sreenivasan[1].

A. The Governing Equations

The dynamics of turbulent mixing are generally described by coupling the Navier-Stokes equations for the velocity field with an advection-diffusion equation for the scalar field[4,6]:

$$\frac{\partial \vec{v}}{\partial t} + (\vec{v}\cdot\vec{\nabla})\vec{v} = -\vec{\nabla}p + \nu\vec{\nabla}^2\vec{v}, \tag{1}$$

$$\vec{\nabla}\cdot\vec{v} = 0, \tag{2}$$

$$\frac{\partial T}{\partial t} + (\vec{v}\cdot\vec{\nabla})T = D\vec{\nabla}^2 T. \tag{3}$$

Here:

- $\vec{v}(x,y,z,t)$ is the fluid velocity vector,
- $p(x,y,z,t)$ is the pressure field,
- $T(x,y,z,t)$ represents the passive scalar field (e.g., concentration, temperature),
- ν is the kinematic viscosity,
- D is the diffusivity of the scalar.

These equations capture essential physics of passive scalar transport in turbulent flows, underpinning analyses in various natural and technological settings[7].

B. Role of Turbulent Mixing in Natural Systems

Turbulent mixing is pivotal in numerous natural phenomena:

Atmospheric Dispersion: Turbulent mixing strongly influences pollutant dispersion, cloud formation, and chemical transformations in the atmosphere, significantly affecting climate and air quality[3].

Oceanographic Processes: Mixing affects nutrient distribution, temperature and salinity gradients, and thereby shapes marine ecosystems and global ocean currents[2].

Geophysical Flows: Heat and chemical transport in Earth's mantle and volcanic systems rely heavily on turbulent mixing, influencing geological activity and tectonic movements[2].

Astrophysical Flows: Turbulent mixing facilitates elemental and thermal transport within stellar interiors, supernovae, and interstellar media, thereby influencing stellar evolution and cosmic chemical enrichment[2].

C. Experimental Studies of Turbulent Mixing

Experiments have greatly advanced our understanding of turbulent mixing:

Scalar Transport Dynamics: Experiments quantify scalar dispersion, validating theoretical predictions and identifying universal mixing behaviors[8].

Mixing Layers and Interfaces: Experimental visualization of turbulent interfaces has clarified interfacial dynamics and scalar entrainment processes[3].

Boundary Effects: Investigations into boundary-driven scalar mixing have enhanced understanding of mixing in environmental and industrial applications[3].

Early experiments: The early paper[9] presents an experimental investigation into the behavior of passive scalar (temperature) fluctuations within nearly isotropic turbulence generated by grids.

This study provides valuable insights into the behavior

of passive scalars in turbulent flows, particularly highlighting how different methods of introducing thermal fluctuations affect the decay and distribution of temperature fluctuations. The findings have implications for understanding mixing processes and scalar transport in turbulent environments.

D. Theoretical Advances in Turbulent Mixing

There was no microscopic theory until now, but some theoretical progress has been achieved in scalar turbulence:

Scaling Laws and Universality: Theoretical predictions link scalar variance and mixing efficiency to turbulence characteristics, notably through assumed universal scaling laws[7].

Instabilities and Structures: Analytical studies identify instabilities and coherent structures driving scalar mixing, elucidating scalar transport mechanisms[3].

Reduced and Phenomenological Models: Simplified models facilitate analytical insights into scalar mixing, capturing essential turbulence-driven dynamics[3].

Kraichnan Model: The Kraichnan model, introduced by Robert H. Kraichnan in 1968, is a cornerstone in the theoretical study of passive scalar turbulence. It considers the advection of a passive scalar field by a Gaussian, statistically homogeneous, and isotropic velocity field that is delta-correlated in time. This model has been instrumental in understanding the anomalous scaling behaviors observed in turbulent flows.

In the comprehensive review,[10] delve into the intricacies of the Kraichnan model, particularly focusing on the decay of passive scalars in turbulent environments. They highlight how the model allows for exact analytical treatments, leading to insights into the scaling exponents and the multifractal nature of scalar fields in turbulence.

The review discusses the emergence of anomalous scaling laws, which deviate from classical Kolmogorov predictions, and attributes these anomalies to the intermittent nature of scalar fluctuations. The authors also explore the role of zero modes and the operator product expansion in determining the scaling behavior of scalar correlation functions.

Furthermore, the paper examines the implications of the Kraichnan model for real-world turbulent systems, emphasizing its relevance in contexts where the velocity field exhibits short correlation times. The insights gained from this model have profound implications for our understanding of mixing and transport processes in turbulent flows.

Nevertheless, this model misses the nonperturbative phenomena, which can only be described by an exact solution of the NS equations. Thus, we treat this work as an insight rather than a source of quantitative information regarding the passive scalar.

E. Applications of Turbulent Mixing

Practical applications of turbulent mixing include:

Environmental Management: Improved pollutant dispersion models guide environmental policy and response strategies[2].

Industrial Processes: Effective turbulent mixing enhances chemical engineering processes, combustion efficiency, pharmaceutical manufacturing, and food processing[2].

Climate Modeling: Better modeling of turbulent mixing refines climate forecasts and global climate change mitigation strategies[2].

F. State of the Art in Numerical Simulations

Direct numerical simulations (DNS) provide critical insights into turbulent scalar mixing:

Scalar Dispersion and Mixing Verification: DNS validates theoretical predictions, significantly refining scalar dispersion models[11].

Multiscale Mixing Analysis: High-resolution simulations reveal interactions across scales, vital for accurate scalar transport modeling[12].

Boundary and Interface Dynamics: DNS captures detailed dynamics at interfaces, crucial for understanding scalar mixing in realistic scenarios[11].

Despite these advancements, computational constraints remain significant, especially in modeling natural systems at realistically high Reynolds and Schmidt numbers, necessitating ongoing developments in computational techniques and resources[11].

II. PASSIVE SCALAR MOTION IN LOOP SPACE

The basic quantity in the loop space approach to fluid dynamics[13–16], is the loop functional:

$$\Psi[C,t] = \left\langle \exp\left(\frac{\imath\Gamma_C[v]}{\nu}\right)\right\rangle; \tag{4}$$

$$\Gamma_C[v] = \oint d\theta \vec{C}'(\theta,t)\cdot\vec{v}(\vec{C}(\theta,t)) \tag{5}$$

We took static loop $\vec{C}(\theta)$ not moving with the flow in these papers. Now we need to modify this definition: we let the loop move with the flow:

$$\partial_t\vec{C}(\theta,t) = \vec{v}(\vec{C}(\theta,t),t) \tag{6}$$

The loop average will then be a functional of the initial value $\vec{C}_0(\theta)$ for this moving loop. The rest of the transformations to the loop space are the same as before. The movement of the loop eliminates one term in the Navier-Stokes equations for the velocity and the temperature, namely the advection term. We find, using the

Navier-Stokes equations

$$\partial_t \Gamma_C[v] = \oint d\theta \vec{C}'(\theta,t)\left(\vec{\nabla}\times\vec{\omega}\right); \tag{7}$$

$$\partial_t T(\vec{C}(\theta,t),t) = D\vec{\nabla}^2 T(\vec{C}(\theta,t),t) \tag{8}$$

The general solution for the passive scalar **on the moving loop** reads

$$T(\vec{C}(\theta,t),t) = \int d^3q W(\vec{q}) \exp\left(-D\vec{q}^2 t + \imath\vec{q}\cdot\vec{C}(\theta,t)\right); \tag{9a}$$

$$W(\vec{q}) = \int \frac{d^3r}{(2\pi)^3}\exp\left(-\imath\vec{q}\cdot\vec{r}\right) T(\vec{r},0); \tag{9b}$$

In particular, for a single delta-source of the heat at the initial moment, $T(\vec{r},0) = T_0\delta(\vec{r})$, we would have $W(\vec{q}) = T_0$.

This solution for T must be combined with the Euler ensemble solution for decaying turbulence[13,14]. In the Lagrangean frame, this solution reads

$$\Psi[C,t] = \left\langle \exp\left(\frac{\imath\oint d\theta\vec{C}'(\theta,t)\cdot\vec{F}(\theta)}{\sqrt{2\nu t}}\right)\right\rangle_{\mathcal{E}}; \tag{10a}$$

$$\vec{C}(\theta,t) = \vec{C}_0(\theta) + \sqrt{2\nu t}\vec{F}(\theta); \tag{10b}$$

$$\vec{F}(\theta) = R\hat{\Omega}\cdot\{\cos\alpha(\theta),\sin\alpha(\theta),0\};\ \hat{\Omega}\in SO(3) \tag{10c}$$

$$\alpha(\theta) = \beta\sum_{l<N\theta/(2\pi)}\sigma_l;\ \sigma_l = \pm 1; \tag{10d}$$

$$R = \frac{1}{2\sin\frac{\beta}{2}}; \tag{10e}$$

$$\beta = \frac{2\pi p}{q};\ \gcd(p,q) = 1; \tag{10f}$$

$$\sum_1^N \sigma_l = rq; r\in\mathbb{Z}; \tag{10g}$$

$$N \mod 2 = 0; \tag{10h}$$

We drop an arbitrary constant t_0 added to the time, so that the initial data is at $t = -t_0$. The averaging $\langle ...\rangle_{\mathcal{E}}$ stands for the averaging over the Euler ensemble $\hat{\Omega},\sigma_1,\ldots,\sigma_N,p,q,r$. The details of the discretization of the loop equation can be found in[15], where the original loop equation for a static loop was derived. The computations of the Euler ensemble averages were performed in[14] (see appendixes and notebooks quoted there for the details).

III. THE CORRELATIONS OF PASSIVE SCALAR

Let us first consider the pair correlation function of the passive scalar moved by the Euler ensemble of decaying turbulence. For an arbitrary moving loop $\vec{C}(\theta,t)$ we have the following correlation function

$$\iint\limits_{0<\theta_1<\theta_2<2\pi}\frac{d\theta_1 d\theta_2}{2\pi^2} \left\langle T(\vec{C}(\theta_1,t),t)T(\vec{C}(\theta_2,t),t)\exp\left(\frac{\imath\Gamma_C[v]}{\nu}\right)\right\rangle_v \tag{11}$$

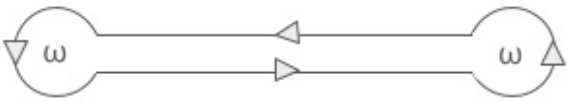

Figure 1. The hairpin loop generating a correlation function with small circles around two points $\vec{r}_1,\vec{r}_2$

The correlation for the static loop we need can be obtained from this one using the translation operator

$$\iint\limits_{0<\theta_1<\theta_2<2\pi}\frac{d\theta_1 d\theta_2}{2\pi^2} \left\langle T(\vec{C}_0(\theta_1),t)\,T(\vec{C}_0(\theta_2),t)\exp\left(\frac{\imath\Gamma_{C_0}[v]}{\nu}\right)\right\rangle_v = \iint\limits_{0<\theta_1<\theta_2<2\pi}\frac{d\theta_1 d\theta_2}{2\pi^2} \left\langle \hat{\mathbb{T}}\,T(\vec{C}(\theta_1,t),t)\,T(\vec{C}(\theta_2,t),t)\exp\left(\frac{\imath\Gamma_C[v]}{\nu}\right)\right\rangle_v; \tag{12}$$

$$\hat{\mathbb{T}} = \exp\left(\oint d\theta\left(\vec{C}_0(\theta)-\vec{C}(\theta,t)\right)\cdot\frac{\delta}{\delta\vec{C}(\theta,t)}\right); \tag{13}$$

Representing this in momentum loop space, we find

$$\hat{\mathbb{T}}\Rightarrow\exp\left(\imath\sqrt{2\nu t}\oint d\theta\vec{F}(\theta)\cdot\vec{P}'(\theta,t)\right) = \exp\left(\imath\oint d\theta\vec{F}(\theta)\cdot\vec{F}'(\theta)\right) = 1; \tag{14}$$

The last equation follows from the periodicity of the vector function $\vec{F}(\theta)$

$$\oint d\theta\vec{F}(\theta)\cdot\vec{F}'(\theta) = \frac{\vec{F}(2\pi)^2-\vec{F}(0)^2}{2} = 0; \tag{15}$$

Therefore, the moving loop has the same statistics as the static one!

We can now substitute the solution for $T(\vec{C}(\theta_i,t),t)$. After some transformations we find

$$\left\langle T(\vec{C}(\theta_1,t),t)T(\vec{C}(\theta_2,t),t)\exp\left(\frac{\imath\Gamma_C[v]}{\nu}\right)\right\rangle_v = \int d^3q_1 d^3q_2 W(\vec{q}_1)W(\vec{q}_2) \exp\left(-\left(\vec{q}_1^2+\vec{q}_2^2\right)Dt + \imath\vec{C}_0(\theta_1)\cdot\vec{q}_1 + \imath\vec{C}_0(\theta_2)\cdot\vec{q}_2\right) \left\langle\exp\left(\imath\oint d\theta\frac{\vec{C}_0'(\theta)\cdot\vec{F}(\theta)}{\sqrt{2\nu t}}\right)\right\rangle_{\mathcal{E}}; \tag{16}$$

Now, like in the hydro case[14] we choose the loop C_0 as a hairpin Fig.1. There is no circulation for this loop, so we have just a product of two scalars averaged over turbulent velocity field on the left side. This correlation function does not depend on θ_1,θ_2, so we can integrate them out.

On the right side, in momentum space, we get our correlation computed in the Lagrangian frame

$$\langle T(\vec{r}_1,t)T(\vec{r}_2,t)\rangle_v = \int d^3q_1 d^3q_2 F(\vec{q}_1)F(\vec{q}_2) \exp\left(-\left(\vec{q}_1^2+\vec{q}_2^2\right)Dt + \imath\vec{r}_1\cdot\vec{q}_1+\imath\vec{r}_2\cdot\vec{q}_2\right) \iint\limits_{0<\theta_1<\theta_2<2\pi} \frac{d\theta_1 d\theta_2}{2\pi^2}\left\langle \exp\left(\imath\oint d\theta \frac{\vec{C}_0'(\theta)\cdot\vec{F}(\theta)}{\sqrt{2\nu t}}\right)\right\rangle_{\mathcal{E}}; \quad (17)$$

Then hairpin loop $\vec{C}_0(\theta)$ is

$$\vec{C}_0(\theta)=\begin{cases}\dfrac{(\theta_2-\theta)\vec{r}_1+(\theta-\theta_1)\vec{r}_2}{\theta_2-\theta_1} & if\ \theta_1<\theta<\theta_2\\ \dfrac{(2\pi+\theta_1-\theta)\vec{r}_2+(\theta-\theta_2)\vec{r}_1}{2\pi+\theta_1-\theta_2} & otherwise\end{cases} \quad (18)$$

The integral here is the same as in the hydro correlation[14]. In present notations

$$\oint d\theta \vec{C}_0'(\theta)\cdot\vec{F}(\theta)=\vec{r}_{12}\cdot\Delta\vec{S}; \quad (19)$$

$$\Delta\vec{S}=\vec{S}(\theta_1,\theta_2)-\vec{S}(\theta_2,2\pi+\theta_1); \quad (20)$$

$$\vec{S}(x,y)=\frac{\int_x^y\vec{F}(\theta)d\theta}{y-x}; \quad (21)$$

$$\vec{r}_{12}=\vec{r}_2-\vec{r}_1; \quad (22)$$

IV. UNIVERSAL SCALING SUNCTION

Let us introduce the scaling variables, measuring the coordinates and momenta in the units of diffusion length $\sqrt{2Dt}$

$$\vec{\rho}_{1,2}=\frac{\vec{r}_{1,2}}{\sqrt{2Dt}}; \quad (23)$$

$$\vec{\kappa}_{1,2}=\vec{q}_{1,2}\sqrt{2Dt} \quad (24)$$

In the new variables, the correlator becomes

$$\langle T(\vec{r}_1,t)T(\vec{r}_2,t)\rangle_v = \iint\frac{d^3\kappa_1 d^3\kappa_2}{(2Dt)^3}W\left(\frac{\vec{\kappa}_1}{\sqrt{2Dt}}\right)W\left(\frac{\vec{\kappa}_1}{\sqrt{2Dt}}\right) \iint\limits_{0<\theta_1<\theta_2<2\pi}\frac{d\theta_1 d\theta_2}{2\pi^2}\exp\left(-\frac{1}{2}\left(\vec{\kappa}_1^2+\vec{\kappa}_1^2\right)+\imath\vec{\rho}_1\cdot\vec{\kappa}_1+\imath\vec{\rho}_2\cdot\vec{\kappa}_2\right) \left\langle\exp\left(\imath\sqrt{D/\nu}(\vec{\rho}_2-\vec{\rho}_1)\cdot\Delta\vec{S}\right)\right\rangle_{\mathcal{E}}; \quad (25)$$

Now, assuming a finite limit $W(\vec{q}\to 0)$ in Fourier space (a normalizable distribution of initial scalar) , we have, at large time, a universal function for scalar correlation

$$\langle T(\vec{r}_1,t)T(\vec{r}_2,t)\rangle_v \to \frac{2W(0)^2}{(4\pi Dt)^3}\iint\limits_{0<\theta_1<\theta_2<1}d\theta_1 d\theta_2\left\langle\exp(A)\right\rangle_{\mathcal{E}}; \quad (26)$$

$$A=-\frac{\vec{\rho}_1^2+\vec{\rho}_2^2}{2}+ \imath\sqrt{D/\nu}(\vec{\rho}_2-\vec{\rho}_1)\cdot\left(\vec{S}(\theta_1,\theta_2)-\vec{S}(\theta_2,2\pi+\theta_1)\right); \quad (27)$$

As anticipated, this correlation function is universal, apart from its dependence on the Schmidt number $Sc=\nu/D$.

The observed correlation function is averaged over translations

$$G(\vec{r},t)=\frac{\int_V d^3r_1\langle T(\vec{r}_1,t)T(\vec{r}_1+\vec{r},t)\rangle}{V}; \quad (28)$$

This integration yields (with $\vec{\rho}=\frac{\vec{r}}{\sqrt{2Dt}}$)

$$G(\vec{r},t)= \frac{W(0)^2}{(2\sqrt{2\pi Dt})^3 V}\iint\limits_{0<\theta_1<\theta_2<2\pi}\frac{d\theta_1 d\theta_2}{2\pi^2}\langle\exp(B)\rangle_{\mathcal{E}}; \quad (29)$$

$$B=-\frac{\vec{\rho}^2}{4}+\imath\frac{\vec{\rho}\cdot\left(\vec{S}(\theta_1,\theta_2)-\vec{S}(\theta_2,1+\theta_1)\right)}{\sqrt{Sc}} \quad (30)$$

We perform the Fourier transformation in $\vec{r}$ and find the scalar spectrum. This is a universal function of a scaling variable $\vec{\kappa}=\vec{q}\sqrt{2Dt}$ and the Schmidt number Sc.

$$g(\vec{k},t)=(2\sqrt{Dt})^3\int d^3\rho\exp(\imath\vec{\kappa}\cdot\vec{\rho})G(\vec{r},t)=\frac{2W(0)^2}{\pi^3 V} \iint\limits_{0<\theta_1<\theta_2<1}d\theta_1 d\theta_2\left\langle\exp\left(-\frac{\left(\Delta\vec{S}+\vec{\Omega}\cdot\vec{\kappa}\sqrt{Sc}\right)^2}{Sc}\right)\right\rangle_{\mathcal{E}}; \quad (31)$$

$$\Delta\vec{S}=\vec{S}(\theta_1,\theta_2)-\vec{S}(\theta_2,1+\theta_1); \quad (32)$$

$$\vec{S}(x,y)=\frac{\int_x^y\vec{F}(\theta)d\theta}{y-x}; \quad (33)$$

Integrating over rotations in 3D reduces to a one-dimensional integral

$$\left\langle\exp\left(-\frac{\left(\Delta\vec{S}+\vec{\Omega}\cdot\vec{\kappa}\sqrt{Sc}\right)^2}{Sc}\right)\right\rangle_{\Omega}= \int_{-1}^1\frac{dz}{2}\exp\left(-\frac{\Delta\vec{S}^2+2z|\Delta\vec{S}||\vec{\kappa}|\sqrt{Sc}+\vec{\kappa}^2Sc}{Sc}\right) \quad (34)$$

V. TURBULENT LIMIT

Turbulent limit in our theory corresponds to vanishing viscosity $\nu\to 0$ at a large number of points $N\to\infty$. Later, we figure out what to do with the diffusivity D in this limit. The sum over Ising variables in the Euler ensemble becomes the path integral over trajectories $\alpha(\theta)$ of the Brownian motion

$$\left\langle\exp\left(-\frac{\left(\Delta\vec{S}+\vec{\Omega}\cdot\vec{\kappa}\sqrt{Sc}\right)^2}{Sc}\right)\right\rangle_{\mathcal{E}}\to \int_{-1}^1\frac{dz}{2}\int dX f_X(X)\int D\alpha(\xi)\exp\left(-\int_0^1 d\xi\frac{(\alpha')^2}{2N\beta^2}\right) \exp\left(-\frac{\Delta\vec{S}^2+2z|\Delta\vec{S}||\vec{\kappa}|\sqrt{Sc}+\vec{\kappa}^2Sc}{Sc}\right); \quad (35)$$

In this section, we use the variable $\xi=\frac{\theta}{2\pi}$ matching the parametrization of the previous work[14].

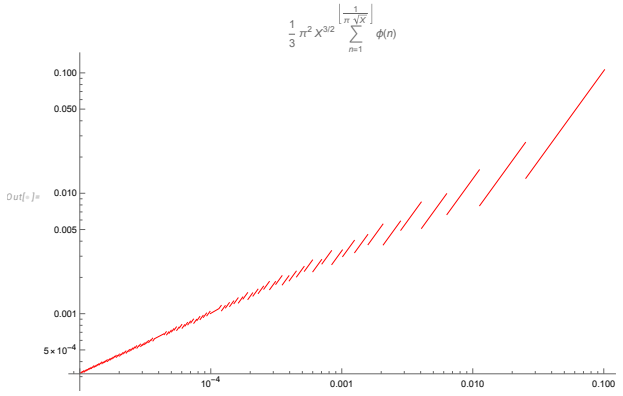

Figure 2. Log log plot of the distribution (37)

In this limit, the typical values of the angle $\beta = 2\pi p/q \sim 1/N \to 0$, so that the radius of the regular star polygons is large

$$R = 1/(2\sin(\pi p/q) \sim N \to \infty \tag{36}$$

The distribution of the variable $X(p,q) = \cot(\pi p/q)^2/N^2 = \left(4R^2-1\right)/N^2$ for large co-prime $1 \geq p < q < N$ was studied in the previous work, and it is a discontinuous piecewise power like distribution

$$f_X(X) = \left(1 - \frac{\pi^2}{675\zeta(5)}\right)\delta(X) + \frac{\pi^3}{3} X\sqrt{X}\Phi\left(\left\lfloor \frac{1}{\pi\sqrt{X}} \right\rfloor\right); \tag{37}$$

depicted in Figure.2. Here $\Phi(n)$ is the totient summatory function

$$\Phi(q) = \sum_{n=1}^{q} \varphi(n) \tag{38}$$

With $R \sim N$, the estimate of $|\Delta\vec{S}|$ would also be $O(N)$, except for the small values of the phase $\alpha(\theta)$. As it was found in[14], this phase goes to zero, $\alpha(\theta) \propto 1/\sqrt{N}$. The average in (34) is a function of

$$|\Delta\vec{S}| = \frac{N\sqrt{X}}{2}\left|\frac{\int_{\xi_1}^{\xi_2} d\xi\, e^{\imath\alpha}}{\xi_2-\xi_1} - \frac{\int_{\xi_2}^{1+\xi_1} d\xi\, e^{\imath\alpha}}{1+\xi_1-\xi_2}\right| \tag{39}$$

At large N we have a saddle point for the path integral over phases α of the Brownian motion. It is convenient to reduce this problem to the one solved in[14] by adding one more integration

$$\left\langle \exp\left(-\frac{\left(\Delta\vec{S} + \vec{\Omega}\cdot\vec{\kappa}\sqrt{Sc}\right)^2}{Sc}\right)\right\rangle_{\mathcal{E}} \propto \int_{-1}^{1}\frac{dz}{2}\exp\left(-\kappa^2(1-z^2)\right)$$
$$\int dX f_X(X)\int_{-\imath\infty}^{\imath\infty} d\lambda \exp\left(\frac{Sc\lambda^2}{4} + \lambda z\kappa\sqrt{Sc}\right)$$
$$\int D\alpha(\xi)\exp\left(-\oint d\xi \frac{(\alpha')^2}{2N\beta^2} - \lambda|\Delta\vec{S}|\right); \tag{40}$$

We observe that in the critical region $\beta \to 0$, we can replace

$$\frac{1}{2N\beta^2} \to \frac{1}{8N}\cot^2\beta/2 = \frac{N}{8}X \tag{41}$$

The leading terms in the exponential (effective action) will be

$$A[\alpha, r] = \frac{X}{4}\int_{\xi_1}^{1+\xi_1}(\alpha')^2 + \lambda\sqrt{X}\left|\frac{\int_{\xi_1}^{\xi_2} d\xi\, e^{\imath\alpha}}{\xi_2-\xi_1} - \frac{\int_{\xi_2}^{1+\xi_1} d\xi\, e^{\imath\alpha}}{1+\xi_1-\xi_2}\right|; \tag{42}$$

up to the common $N/2$ factor. This variational problem at fixed λ was solved in[14]. In the present notations and normalization

$$\alpha_1'' + \frac{r}{\xi_2-\xi_1}\sin\alpha_1 = 0; \forall\xi_1 < \xi < \xi_2 \tag{43}$$
$$\alpha_2'' + \frac{r}{\xi_2-\xi_1-1}\sin\alpha_2 = 0; \forall\xi_2 < \xi < 1+\xi_1 \tag{44}$$
$$I(r) = \left|\frac{\int_{\xi_1}^{\xi_2} d\xi\, e^{\imath\alpha}}{\xi_2-\xi_1} - \frac{\int_{\xi_2}^{1+\xi_1} d\xi\, e^{\imath\alpha}}{1+\xi_1-\xi_2}\right|; \tag{45}$$

This equation is solvable in terms of elliptic amplitudes (the pendulum eqution)[17]. We, however, only need a linear approximation at $N \to \infty$, when $\sin\alpha_i \to \alpha_i$ The corresponding solution with matching values and derivatives at $\xi = \xi_1, \xi_1+1$ and $\xi = \xi_2$ reads (up to overall normalization factor a which we determine later)

$$\alpha_1(\xi) = \cos\left(K_1(\xi-\xi_2)\right) + \frac{b}{K_1}\sin\left(K_1(\xi-\xi_2)\right); \tag{46}$$
$$\alpha_2(\xi) = \cos\left(K_2(\xi-\xi_2)\right) + \frac{b}{K_2}\sin\left(K_2(\xi-\xi_2)\right); \tag{47}$$
$$K_1 = \sqrt{\frac{r}{\Delta}}; \tag{48}$$
$$K_2 = \sqrt{\frac{r}{\Delta-1}}; \tag{49}$$
$$\Delta = \xi_2 - \xi_1; \tag{50}$$

In the physical region $r > 0$, K_1 is real, and K_2 is imaginary, but the solution stays real. The matching conditions at $\alpha_1(\xi_2) = \alpha_2(\xi_2), \alpha_1'(\xi_2) = \alpha_2'(\xi_2)$ are identically satisfied with this Anzatz. The derivative match $\alpha_1'(\xi_1) = \alpha_2'(1+\xi_1)$ can be solved exactly for b

$$b = \frac{P}{Q}; \tag{51}$$
$$P = \sqrt{\frac{r}{\Delta-1}}\sin\left((1-\Delta)\sqrt{\frac{r}{\Delta-1}}\right) + \sqrt{\frac{r}{\Delta}}\sin\left(\Delta\sqrt{\frac{r}{\Delta}}\right); \tag{52}$$
$$Q = \cos\left((\Delta-1)\sqrt{\frac{r}{\Delta-1}}\right) - \cos\left(\Delta\sqrt{\frac{r}{\Delta}}\right) \tag{53}$$

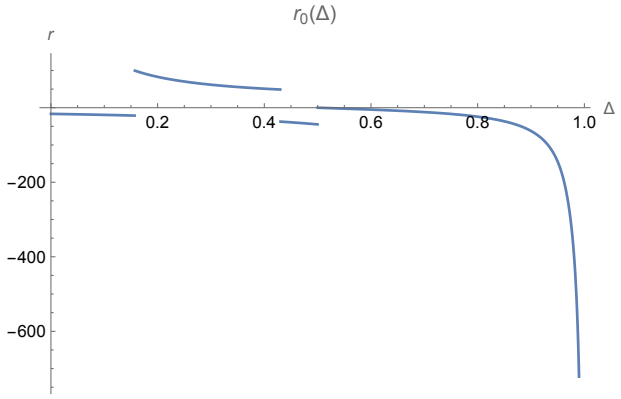

Figure 3. The parameter $r(\Delta)$ as a function of $\Delta = \xi_2 - \xi_1$

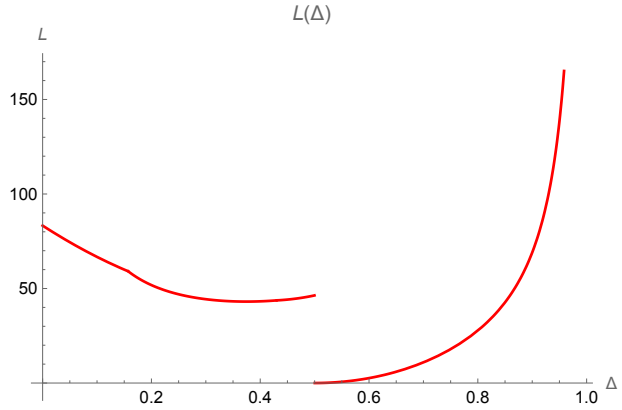

Figure 4. The kinetic energy (57) as a function of $\Delta = \xi_2 - \xi_1$

The remaining matching condition $\alpha_1(\xi_1) = \alpha_2(1+\xi_1)$ reduces to the root of the function

$$g(r,\Delta) = \frac{(2\Delta-1)\sin\left(\sqrt{(\Delta-1)r}\right)\sin\left(\sqrt{\Delta r}\right)}{\sqrt{(\Delta-1)\Delta}} + 2\cos\left(\sqrt{(\Delta-1)r}\right)\cos\left(\sqrt{\Delta r}\right) - 2 \tag{54}$$

This function has multiple roots, but we are looking for the real positive root $r_0(\Delta)$ with minimal value of the action at given Δ.

We prove in[17] that the leading linear term of the expansion of $I(r)$ in α vanishes so that $I(r) \sim a^2 \to 0$ The resulting integrals can be expressed as a function of Δ on the roots of $g(r,\Delta)$.

$$I(r)|_{g(r,\Delta)=0} = a^2 S(\Delta); \tag{55}$$

$$S(\Delta) = \left| \frac{\int_{\xi_1}^{\xi_2} d\xi\ \alpha_1^2}{2(\xi_2-\xi_1)} - \frac{\int_{\xi_2}^{1+\xi_1} d\xi\ \alpha_2^2}{2(1+\xi_1-\xi_2)} \right|; \tag{56}$$

$$\int_{\xi_1}^{1+\xi_1} (\alpha')^2 \Big|_{g(r,\Delta)=0} = a^2 L(\Delta); \tag{57}$$

(58)

This universal function $L(\Delta)$ was computed in[18], but the expression is too lengthy to present here. These three universal functions are plotted in Figs. 3,4,5.

Collecting all the terms in the exponential, we find an effective Action (with $L(\Delta) \equiv L, S(\Delta) \equiv S$)

$$\exp\left(-A_{eff}\right); \tag{59}$$

$$A_{eff} = \frac{1}{8}a^2 LNX + \lambda\left(\frac{1}{2}a^2 NS\sqrt{X} - \kappa\sqrt{Sc}z\right) - \frac{\lambda^2 Sc}{4} + \kappa^2\left(1-z^2\right) \tag{60}$$

where $a \sim 1/N$ is the normalization of our solution.

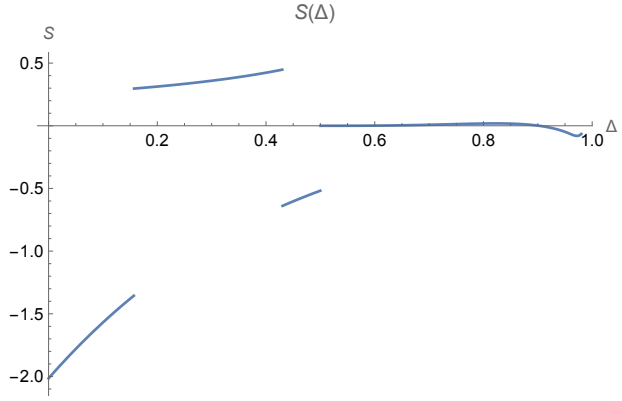

Figure 5. The integral (56) as a function of $\Delta = \xi_2 - \xi_1$

Integrating by λ, we find

$$\frac{2\sqrt{\pi}}{\sqrt{Sc}}\exp\left(-B_{eff}\right); \tag{61}$$

$$B_{eff} = \frac{a^2 NX\left(2a^2 NS^2 + LSc\right)}{8Sc} - \frac{a^2\kappa NS\sqrt{X}z}{\sqrt{Sc}} + \kappa^2 \tag{62}$$

The subsequent integral over a is dominated by a saddle point minimizing B_{eff}.

$$\frac{2\sqrt{\pi}}{\sqrt{Sc}}\exp\left(-\min_a B_{eff}\right); \tag{63}$$

$$\min_a B_{eff} = -\frac{L^2 ScX}{64S^2} + \frac{\kappa L\sqrt{Sc}\sqrt{X}z}{4S} - \kappa^2\left(z^2-1\right); \tag{64}$$

$$a_{min} = \frac{\sqrt{8\kappa S\sqrt{Sc}\sqrt{X}z - LScX}}{2\sqrt{N}S\sqrt{X}} \tag{65}$$

The physical region of the stable solution with $r(\Delta) > 0, S(\Delta) > 0$ is

$$\Delta_1 < \Delta < \Delta_2; \tag{66}$$

$$\Delta_1 = 0.157143; \tag{67}$$

$$\Delta_2 = 0.43015; \tag{68}$$

There is an extra condition of positivity of the expression inside the square root in the solution for a:

$$\sqrt{X} < \frac{8z\kappa S(\Delta)}{L(\Delta)\sqrt{Sc}}; \tag{69}$$

The remarkable property of this computation is that in the end all the dependence of N disappeared in effective Action B_{eff} after minimization. In other words, we found the finite statistical limit of our correlation function in the classical approximation to the effective string theory.

VI. THE FUNCTIONAL DETERMINANT AND MELLIN TRANSFORM

The complete WKB computation also involves the pre-exponential factor coming from the functional determinant of the quadratic form for harmonic deviations from the classical solution. The same problem was already solved in the previous work[14], so we can use the result of this tedious calculation (Appendix I, equations I21, I25). In our case, this functional determinant multiplies the result of the previous WKB computations. This results in the following analytic formula.

$$g(\vec{k},t) \propto$$
$$\int_0^1 dz \exp\left(\kappa^2(z^2-1)\right) \int_{\Delta_1}^{\Delta_2} d\Delta \, \frac{(1-\Delta)Q_\alpha(\Delta,1)}{(\sqrt{Sc}H(\Delta))^{11/2}}$$
$$\sum_{n=1}^{\infty} \varphi(n) \int_0^{x_{min}(n)} dx x^{9/2} \exp\left(\frac{x^2}{4} - z\kappa x\right); \tag{70a}$$
$$\kappa = |\vec{k}|\sqrt{2D(t+t_0)}; \tag{70b}$$
$$H(\Delta) = \frac{L(\Delta)}{4S(\Delta)}; \tag{70c}$$
$$x_{min}(n) = \min\left(\frac{\sqrt{Sc}H(\Delta)}{\pi n}, 2\kappa z\right); \tag{70d}$$

Technically, this can be declared as a solution in quadrature, as the function $Q_\alpha(\Delta,1)$ was reduced in[14] to sums of integrals of elementary functions in Appendix I, eqs(I21, I16, I13, I14). Using *Mathematica*®, we managed to tabulate the universal functions $H(\Delta), Q_\alpha(\Delta,1)$ and this allows us to compute the spectrum for a range of values of Sc. (see Fig. 6 , 7).

The general formula (70) can be transformed to a Mellin integral, which is suitable for the computation of the spectrum of decay indexes. As we have done in Appendix K in[14], we represent the step function as a Mellin integral:

$$\theta\left(\frac{\sqrt{Sc}H(\Delta)}{\pi n x} - 1\right) =$$
$$\int_{c-\imath\infty}^{c+\imath\infty} \frac{dp}{2\pi\imath p} \left(\frac{\sqrt{Sc}H(\Delta)}{\pi x}\right)^p n^{-p} \tag{71}$$

where $c > 2$ to provide convergence of the sum over n

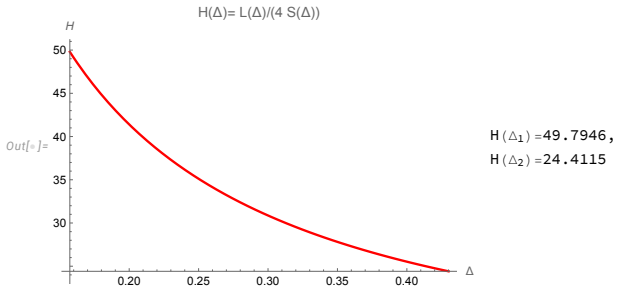

Figure 6. The function $H(\Delta)$ as a function of $\Delta = \xi_2 - \xi_1$

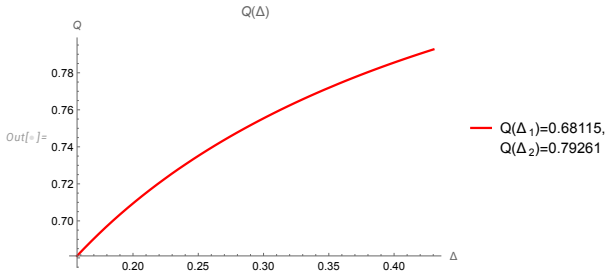

Figure 7. The universal function $Q(\Delta) = Q_\alpha(\Delta,1)$ as a function of $\Delta = \xi_2 - \xi_1$

below. This sum reduces to a ratio of two zeta functions:

$$\sum_{n=1}^{\infty} \varphi(n) \int_0^{x_{min}(n)} dx x^{9/2} \exp\left(\frac{x^2}{4} - z\kappa x\right) =$$
$$\int_{c-\imath\infty}^{c+\imath\infty} \frac{dp}{2\pi\imath} \frac{\zeta(p-1)}{p\zeta(p)} \left(\frac{\sqrt{Sc}H(\Delta)}{\pi}\right)^p$$
$$\int_0^{2\kappa z} dx x^{9/2-p} \exp\left(\frac{x^2}{4} - z\kappa x\right); \tag{72}$$

We introduce a holomorphic function

$$f(\omega) = Sc^{\omega/2} \int_{\Delta_1}^{\Delta_2} d\Delta \, (1-\Delta)Q_\alpha(\Delta,1) \left(\frac{H(\Delta)}{\pi}\right)^\omega; \tag{73}$$

This is an entire function, because the factor $H(\Delta)$ varies in finite positive limits, and so does the other factor $Q_\alpha(\Delta,1)$. Using these properties, one may prove convergence of the Taylor series in ω around the origin.

Now we rewrite the integral as follows:

$$\int_{c-\imath\infty}^{c+\imath\infty} \frac{dp}{2\pi\imath} \frac{\zeta(p-1)}{\zeta(p)p} f\left(p - \frac{11}{2}\right)$$
$$\int_0^1 dz \exp\left(\kappa^2(z^2-1)\right) \int_0^{2\kappa z} dx x^{9/2-p} \exp\left(\frac{x^2}{4} - z\kappa x\right) \tag{74}$$

The last double integral can be expanded in an asymptotic series in inverse powers of κ at $\kappa \to \infty$. For this,

we have to replace $z = 1 - \epsilon$ and expand

$$\exp\left(\kappa^2((1-\epsilon)^2 - 1) - (1-\epsilon)\kappa x\right) = \exp\left(-2\epsilon k^2 - \kappa x\right) \sum_n \frac{\kappa^{2n}\epsilon^{2n}}{n!} \sum_m \frac{(\epsilon\kappa x)^m}{m!}; \quad (75)$$

$$\exp\left(\frac{x^2}{4}\right) = \sum_l \frac{(x/2)^{2l}}{l!} \quad (76)$$

The resulting integrals will reduce to the Γ function and powers of κ, if we set to $+\infty$ the upper limit of the x integral. This will produce an asymptotic expansion of the Mellin function, with each term producing a series of poles, leading to powers of κ in the asymptotic. There are the exponential terms, coming from the upper limit, which we replaced by $+\infty$.

The poles come from the remaining factor $\frac{\zeta(p-1)}{p\zeta(p)}$ leading to the following set of decay powers κ^z

$$z = \left\{-2j - \frac{11}{2}, -2j \pm \imath t(k) - 7, -2j - \frac{17}{2}\right\}; \quad (77)$$

$$j \in \mathbb{Z}, j \geq 0; \quad (78)$$

where $\pm t(k), k = 1, 2, \ldots$ are imaginary parts of nontrivial zeros of the zeta function at $z = 1/2 + \imath t$.

The leading term is proportional to $Sc^{-11/4}\kappa^{-11/2}$, but the sub-leading coefficients have nontrivial dependence on Sc, involving superposition of various powers of Sc, including complex-conjugate powers coming from the zeta zeros.

This strong Sc dependence may lead to the regime changes, like the ones observed in simulations below.

VII. DISCUSSION

The leading term of the passive scalar spectral function (including the additional volume factor in Fourier space) exhibits the following asymptotic decay:

$$E_T(k,t) = 4\pi\vec{k}^2 g(\vec{k},t) \sim Sc^{-11/4}|\vec{k}|^{-7/2}t^{-11/4}. \quad (79)$$

Although no universally accepted value exists for the decay power index, the deep inertial-diffusive region is commonly described by the Kolmogorov–Obukhov–Corrsin (KOC) law $k^{-17/3}$. Our theoretical prediction of $k^{-7/2}$ differs from this model. The numerically simulated spectrum shown in Fig. 8 is reproduced from open source paper[19] .

Instead of the full DNS based on NS equation, this paper used so-called EDQNM simulations, where the fourth moments of velocity were approximated by products of second order terms, like in a Gaussian distribution. This approximation leads to uncontrollable errors, so that these results have no quantitative value.

The influence of the Schmidt number Sc on the observed spectrum remains unquantified. The spectrum clearly changes with Sc, but whether this variation affects the power index or merely reshapes the entire spectrum is not clear. The asymptotic rapid decay looks universal, but more data is needed to measure it with precision and verify its universality.

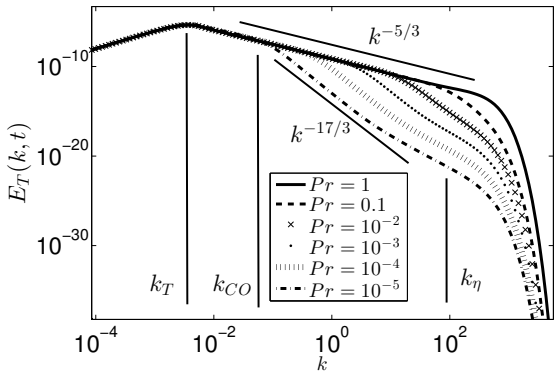

Figure 8. Scalar decay for various Schmidt numbers, from the paper[19]. The curves with various Sc (denoted here as Pr) all converge at large arguments to the same universal rapid decay, approximated by a KOC model $k^{-17/3}$

Our theory proposes that the entire set of decay indices defined in Eq. (77) is universal and composed of half-integer numbers, plus complex-conjugate powers coming from zeros of the zeta function, similar to the hydrodynamic case analyzed in[14].

Nevertheless, the shape of the spectral function given by Eq. (70) strongly depends on Sc via the power of Sc in front of the entire function $f(\omega)$ in (73).

It would be worthwhile to undertake a comprehensive analysis comparing an extensive set of DNS data for passive scalar mixing against our theory across a broad range of Schmidt numbers.

VIII. CONCLUSIONS

As expected, the passive scalar problem reduces to the same random walk on regular star polygons previously encountered in hydrodynamic (HD) and magnetohydrodynamic (MHD) turbulence. A critical insight involves employing the statistical distribution of circulation around a passive loop that moves with the flow. When projected onto this moving loop, the passive scalar diffuses exactly as it would without a flow. Another observation is that the loop functional for a moving loop in decaying turbulence is the same as the one for the initial shape of this loop.

By combining these observations, we obtained the exact analytical solution described in Eqs. (9) and (10). The subsequent computation of the scalar spectrum outlined in Eq. (70) employed the same methodological approach detailed in[14]. The derived asymptotic decay law Eq. (79) differs from the classical KOC model (17/3).

The actual observed spectrum, depicted in Fig. 8, deviates from a linear log-log slope even within the "inertial-

diffusive region." Thus, the complete nonperturbative result given by Eq. (74) should ideally be utilized, with numerical integrations computed via *Mathematica*.

This numerical investigation will form the core of our subsequent study, which aims to rigorously validate the theory against comprehensive DNS and experimental data.

IX. ACKNOWLEDGEMENTS

We benefited from discussions of this work with Semon Rezchikov, Katepalli Sreenivasan, and James Stone. Special thanks to Edoardo Spezzano, who pointed out the correct value of the shift c of the integration contour, leading to extra powers in the decay spectrum.

This research was supported by the Simons Foundation award ID SFI-MPS-T-MPS-00010544 in the Institute for Advanced Study.

REFERENCES

[1] Katepalli R. Sreenivasan. Turbulent mixing: A perspective. *Proceedings of the National Academy of Sciences*, 116(37):18175–18183, 2019.

[2] Paul E Dimotakis. Turbulent mixing. *Annual Review of Fluid Mechanics*, 37:329–356, 2005.

[3] Zellman Warhaft. Passive scalars in turbulent flows. *Annual Review of Fluid Mechanics*, 32:203–240, 2000.

[4] Stephen B Pope. *Turbulent flows*. Cambridge University Press, 2000.

[5] Hendrik Tennekes and John L. Lumley. *A first course in turbulence*. MIT Press, 1972.

[6] Marcel Lesieur. *Turbulence in fluids*. Springer Science & Business Media, 2008.

[7] Boris I Shraiman and Eric D Siggia. Scalar turbulence. *Nature*, 405(6787):639–646, 2000.

[8] Brian Sawford. Turbulent relative dispersion. *Annual Review of Fluid Mechanics*, 33:289–317, 2001.

[9] K. R. Sreenivasan, S. Tavoularis, R. Henry, and S. Corrsin. Temperature fluctuations and scales in grid-generated turbulence. *Journal of Fluid Mechanics*, 100(3):597–621, 1980.

[10] G. Falkovich, K. Gawędzki, and M. Vergassola. Particles and fields in fluid turbulence. *Rev. Mod. Phys.*, 73:913–975, Nov 2001.

[11] Toshiyuki Gotoh and Pui-Kuen Yeung. Passive scalar transport in turbulence: a computational perspective. *Fluid Dynamics Research*, 45(6):061409, 2013.

[12] D. Buaria, A. Pumir, E. Bodenschatz, and P. K. Yeung. Extreme events in scalar turbulence. *Physical Review Letters*, 124(16):164501, 2020.

[13] Alexander Migdal. To the theory of decaying turbulence. *Fractal and Fractional*, 7(10):754, Oct 2023.

[14] Alexander Migdal. Quantum solution of classical turbulence: Decaying energy spectrum. *Physics of Fluids*, 36(9):095161, 2024.

[15] Alexander Migdal. Fluid dynamics duality and solution of decaying turbulence. `https://arxiv.org/abs/2411.01389`, 2024.

[16] Alexander Migdal. Dual theory of mhd turbulence. `https://arxiv.org/abs/2503.12682`, 2025.

[17] Alexander Migdal. "instantoncomputations". "https://www.wolframcloud.com/obj/sasha.migdal/Published/DualTheory2.nb", 03 2024.

[18] Alexander Migdal. "instantoncomputations". "https://www.wolframcloud.com/obj/sasha.migdal/Published/DualTheory1.nb", 03 2024.

[19] Antoine Briard, Thomas Gomez, Pierre Sagaut, and Souzan Memari. Passive scalar decay laws in isotropic turbulence: Prandtl number effects. *Journal of Fluid Mechanics*, 784:274 – 303, November 2015.